POLITECNICO DI MILANO

Scuola di Ingegneria Industriale e dell'Informazione

Corso di Laurea Magistrale in Ingegneria Fisica

Development and study of non-volatile resistive memories based on graphene oxide

Supervisor :
Prof. Riccardo Bertacco

Master Thesis
Florian Robard
matr. 780160

Academic year 2013-2014

Abstract

This work has been about developing and studying a promising type of memory : non-volatile resistive memories based on graphene oxide. Non-volatile memories have been identified as a key device for the future of computational systems considering their reduced energy consumption compared to volatile memories. Graphene related materials offer an interesting and rising alternative to existing technologies.
We have carried out the making of such memories, which are composed of several thin films stacked on a silicon substrate, and examined the fabrication process. To ensure we had mastered the process, we have controlled the thickness of the deposited graphene oxide layer and its roughness. Then we have performed electric characterizations of the fabricated devices and observed that a switching mechanism occured in these structures.

Questo studio consisteva nello sviluppare e analizzare un tipo di memorie promettente : le memorie resistive non-volatili fatte di ossido di grafene. Le memorie non volatili sono state identificate come dei dispositivi chiave per il futuro dei sistemi informatici considerando il consumo energetico ridotto rispetto alle memorie volatili. I materiali legati al grafene offrono un' alternativa interessante e molto promettente alle tecnologie esistenti.
Abbiamo realizzato la fabbricazione di queste memorie, che sono composte di diversi film sottili impilati su uno substrato di silicio, e abbiamo esaminato il processo di realizzazione. Per essere sicuri di dominare il processo, abbiamo controllato lo spessore dello strato di ossido di grafene depositato e la sua ruvidità. Poi abbiamo realizzato delle caratterizzazioni elettriche dei dispositivi fabbricati e abbiamo osservato che un meccanismo di switch si svolge in queste strutture.

Index

Introduction

This work has been carried out at the Thales Research & Technology (TRT) facility in Palaiseau, south of Paris, within the research joint-unit UMR137, which is a laboratory born from a private/public collaboration (Thales/CNRS). My internship there has been an introduction to scientific research and also to a research environment. My task has been influenced by the dual nature of the laboratory in which I was hosted. Indeed its purpose is trying to make a bridge between fundamental research and more applied one. The project has been about the study, fabrication and testing of a type of non-volatile RRAM memories, called « atomic switches » and based on a material called graphene oxide (GO). One of the fabrication steps has been performed thanks to a process patented by my main supervisor there, Paolo Bondavalli, head of the nanomaterial topic team in the joint unit UMR137 Thales/CNRS. My other supervisor, who helped me to proceed the testing part of the work, Julie Grollier, CNRS researcher in the joint team, is a scientist interested among other things in artificial neurons networks, and the non-volatile RRAM memory could provide an important help for the development of such systems.

The RAM memories constitute a huge market shared by many companies. It is commonly stated that the « perfect » memory does not exist yet. This is related to the fact that memories can be characterized by a lot of specific performances : consumption, volatility, writing/reading speed, occupied space (scalability), flexible behaviour, compatibility with CMOS, etc… Different kind of resistive based memories have been developed and each one has its specific advantage. Flash memories offer an interesting compromise between velocity, consumption, non-volatility. Dynamic random access memory (DRAM) are compact and low-cost but don't offer non-volability, which means higher consumption. With a lot of research going on, magnetic random access memory (MRAM) could be the new memory to establish a standard, even if up to now no commercial products have been released. Our work will be focused on RRAM (resistive random access memory), which are also a promising field of research & development considering the lower cost and easy industrial implementation in case of a specific application.

Historically, electrical circuits were crafted with three basic building blocks: the capacitor, the resistor, and the inductor. But in 1971, University of California at Berkeley professor Leon Chua predicted the existence of a fourth: the memristor, short name for memory resistor. Like an ordinary resistor, a memristor would create and maintain a safe flow of electrical current across a device, but unlike a resistor, it would « remember » charges even when the power is turned off. This would allow it to store information in a non-volatile way. More recently in 2011, Leon Chua has stated that the memristor definition could be generalized to cover all forms of 2-terminal non-volatile memory devices based on resistance switching effects.

In electronics, graphene is rapidly becoming the great hope for replacing and improving silicon semiconductors for future high performance devices. Since silicon semiconductors remain the basis of most commercial electronics, especially computing, the challenge for the next generation materials is really huge. The graphene potentialities are attracting a lot of research funding. Another approach currently under development by some teams, and our approach, is to employ graphene and other related nanomaterials to achieve non-volatile memories exploiting their memresistive behaviour.
A large variety of solid-state materials have been found to show these resistive switching characteristics, including solid electrolytes such as GeSe and Ag2S, perovskites such as SrZrO3, and $BiFeO_3$, binary transition metal oxides such as NiO, TiO2, ZrO2, and ZnO, organic materials, amorphous silicon (a-Si), and amorphous carbon (a-C).
The main advantages of graphene related materials are not only that they seem to show extremely promising performances, but also that these materials provide more flexibility (physically) and potentially can lower the final cost of the devices, if scalable fabrication methods are developed in parallel. Moreover we need only a two terminal device, which dramatically reduces the circuitry and allows the implementation of 3D architectures. Finally, this type of circuit commonly used for computer memory could be potentially easily printed or deposited (e.g. by spray-gun) on plastic sheets and used wherever flexibility is needed, such as in wearable electronics.

In this context, my work has had to deal with a graphene-related nanomaterial which is graphene oxide, for the fabrication of non volatile resistive memories (considered memristors). This internship has been part of the beginning of a new research activity on these memories, made of several thin films on a silicon substrate. My goal has been to check the spraying of a uniform layer of graphene oxide, via controlling the influence of its production parameters, i.e. the number of iterations the deposition program was executed, and the graphene oxide concentration in the sprayed solution. We have managed to ensure that this was controlled and have determined that the deposited graphene oxide layer thickness varies linearly with these parameters. After finishing this step, we have carried out the rest of the fabrication of the devices. Indeed after the graphene oxide deposition, we have had to make the metallic square top contacts. These have been made to allow electric characterizations of the devices fabricated, by putting the tip of the testing machine on them. We have found that a switching mechanism occured in some of the fabricated devices, the ones electrochemically active, but not in a reproducible way yet.

Chapter 1

RRAM memories based on graphene oxide

1.1 RRAM memories

RRAM memories (Resistive Random Access Memory) are a non-volatile type of RAM memories. Their operating principle is to induce a switch in a material's resistance to be able to identify different resistance states (ON/OFF). They are generally mainly composed of a three-layer thin film made of metal-insulator-metal materials (see figure 1). Different types of RRAM memories have been tested, mostly different by the type of insulating material used.

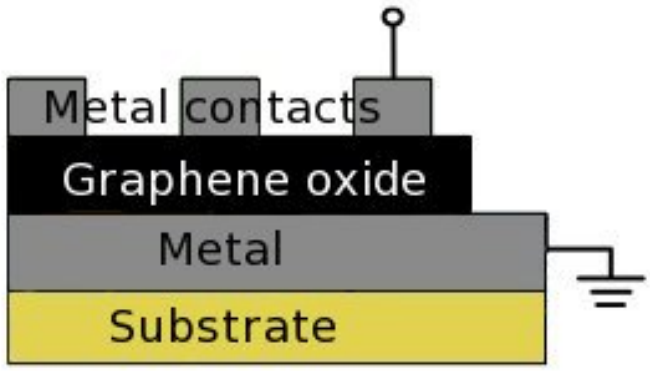

Figure 1 : *Metal-Insulator-Metal structure for a RRAM memory*
Here : insulator material is graphene oxide like in the devices we fabricated

1.1.1 Unipolar / Bipolar RRAM

We have been interested in M-I-M structures, which are metal-insulator-metal structures, with graphene oxide as an insulator. To get the memorization effect, a switch in the structure's resistance that could be detected is required. This switch has to be permanent, so that to remain even when the device is not powered anymore.

Voltage sweeping experiments suggest that for this kind of devices, there are two main behaviours describing the electrical polarity required for resistively switching metal-insulator-metal (MIM) structures. It can be either unipolar or bipolar switching. It is called unipolar (or symmetric) when the switching procedure does not depend on the polarity of the voltage and current signal. A system in its high-resistance state (considered "OFF") is switched ("set") by a threshold voltage into the low-resistance state ("ON"), as sketched in figure 2. In this case, the set voltage is always higher than the reset voltage, and the reset current is always higher than the compliance current (CC), which is the highest current set to prevent the destruction of the device, during set operation. A bipolar switching mechanism will have its set polarity taking place on one polarity of the voltage, and the reset operation requires the opposite polarity. Depending on the specific structure, the curves vary considerably.

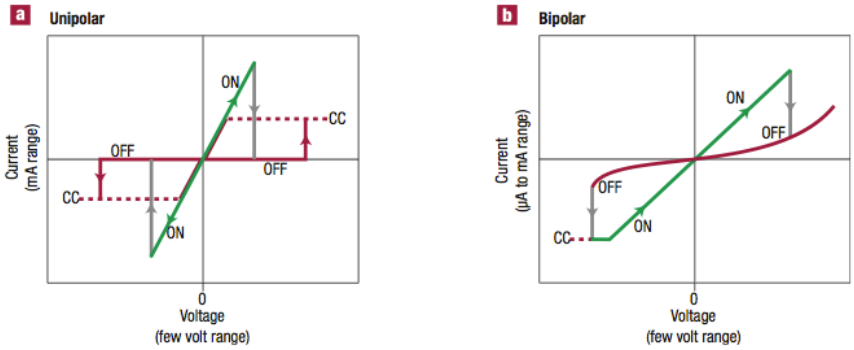

Figure 2 : *The two switching mechanisms in a voltage sweeping experiment*
Left : Unipolar switching / Right : Bipolar switching
Dashed lines indicate that the real voltage at the system will differ from the control voltage because of the compliance current (CC) in action

1.1.2 RRAM atomic switches : redox processes induced by anion-migration

Considering the operating principle of RRAM, there are more than one single phenomenon at the base of the switching mechanism. Furthermore the inside nature of the microscopic processes involved makes it very hard to find adapted instruments or characterization techniques to identify all the right information.

But some scientists are trying to tackle this challenge, accumulating knowledge about the different aspects of the problem trying to elaborate a more complete and accurate model. In this context we have to highlight the work of Rainer Waser about this [2] [3].

The type of mechanism that have been identified to be at stake for graphene oxide based RRAM memories involves redox processes induced by anion-migration. This type of memory is also called **atomic switches**.

In many oxides used as insulator materials in the MIM structures, in particular in transition metal oxides like T_iO_2, oxygen ions defects, typically oxygen vacancies, are much more mobile than cations. If the cathode blocks ion exchange reactions during an electroforming process, an oxygen-deficient region starts to build and to expand towards the anode. Transition metal cations accommodate this deficiency by trapping electrons emitted from the cathode. This virtual cathode moves towards the anode and will finally form a conductive path. At the anode, the oxidation reaction may lead to the liberation of oxygen gas.

Sometimes there is an electroforming step for the conductive filament to form for the first time. This means we have had to put the M-I-M structure under high voltages to activate the conduction path.

1.2 Graphene oxide RRAM memories

1.2.1 The insulator material

Graphene oxide is a wide band gap material, 6eV, with potential for modulation thanks to its oxidation / reduction mechanism providing tunability of the electronics, mechanical, optical properties. Graphene oxide is commonly obtained by oxidation of graphite using the modified Hummer's method [4] [5], where the long oxidation time is combined with a highly effective methods for the purification of reaction products.
Thanks to its high solubility in water, graphene oxide flakes can be put in stable solutions quite easily and deposited on large surface using simple methods such as spray coating or drop casting ; in this work we used another technique, spraying, which will be explained later on.

Graphene oxide remains unfortunately not very well understood or modelized. Regarding its structure for example, several models were proposed but not with great success, see figure 3.

In our experiments we have used a dispersion of graphene oxide sheets from Graphenea. It is obtained from graphite, which is chemically processed to obtain monolayer flakes of graphene oxide.
The sheets were diluted into water and had a 4 g/L concentration, we have then diluted the solution for the sake of the experiments.

1.2.2 The current investigation of graphene oxide memories mechanisms

Previous works have made become graphene oxide a promising solution for fabricating RRAM memories after achieving graphene oxide based M-I-M structures. We have analysed a part of it before starting our own work. Two of the most interesting works have been performed by S.K. Hong [6] and C.L. He [7]. In their article, Hong et al. have investigated the physical explanation of the phenomenon. They tried to deeply understand the mechanism of switching of this kind of devices.

They fabricated several M-I-M devices, with Au and Al as top contacts and graphene oxide as an insulator, and managed to find some elements that could help the understanding of the phenomenon at stake during the switching of the devices. They also made studies varying the materials of the bottom and top electrodes to understand which materials could better work with graphene oxide to obtain optimized devices.
It would seem that the switching operation is influenced by dual mechanism of oxygen migration and top-electrode diffusion into the graphene oxide.

Using a device with an aluminium top contact, they evaluated the effect of the migration of oxygen versus the formation of Al based filaments, and stated that the formation of conducting filaments was a local phenomenon and that the oxygen migration was the dominant mechanism. Indeed they discovered that the leakage current between the bottom and top electrodes was dependent on the cell size. In fact when the cells were

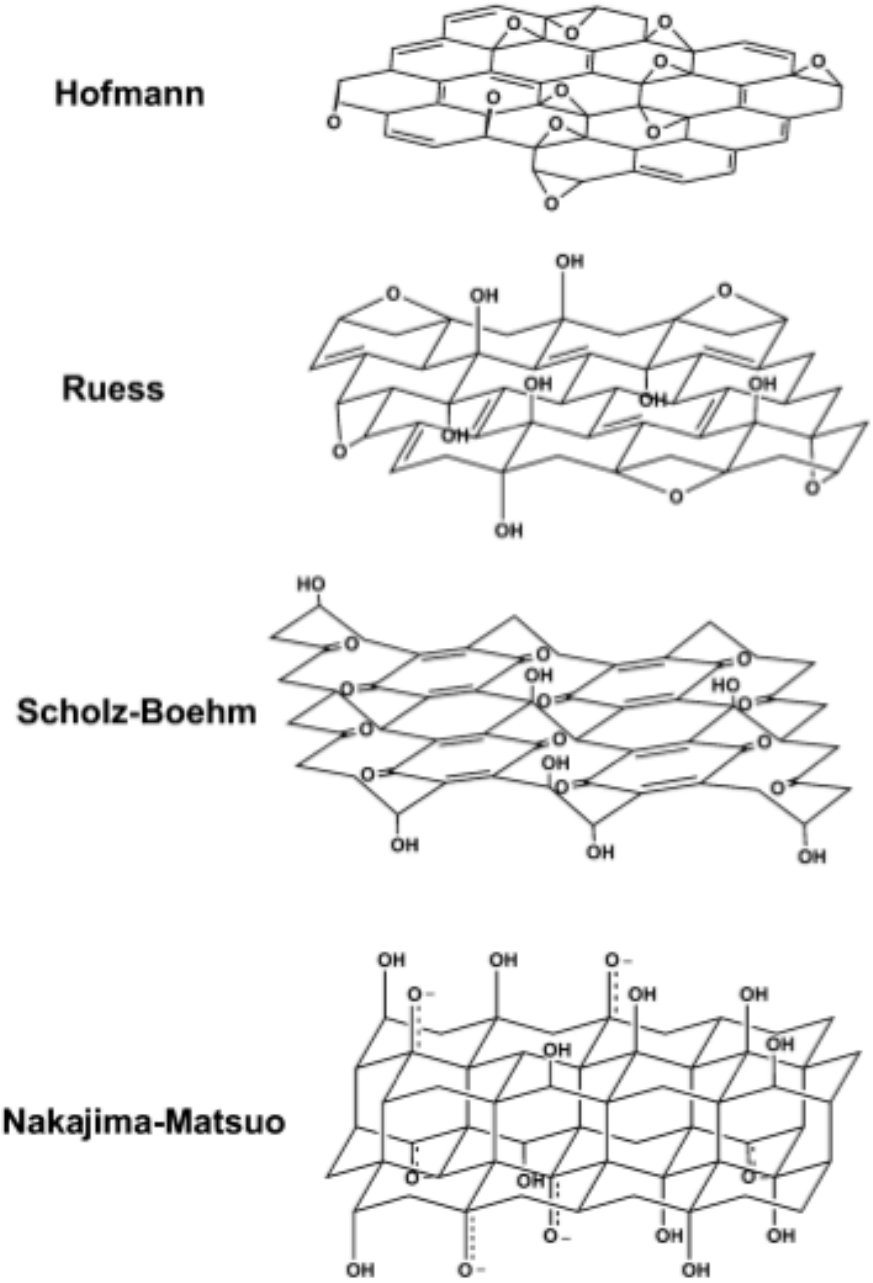

Figure 3 : *Several structural models of graphene oxide*

larger, the effect of the oxygen migration or reduction on the conduction was enhanced, proportionally to the surface.

Hong et al. have also underlined that these structures had performances dependent on the material of the top contacts, probably to its electrochemical behavior. For example, among the devices they tried, in case of Au based top electrodes there was no oxygen migration as in case of Al. Figure 4 displays a result extracted from Hong's article with an electrochemically active top contact (Al).

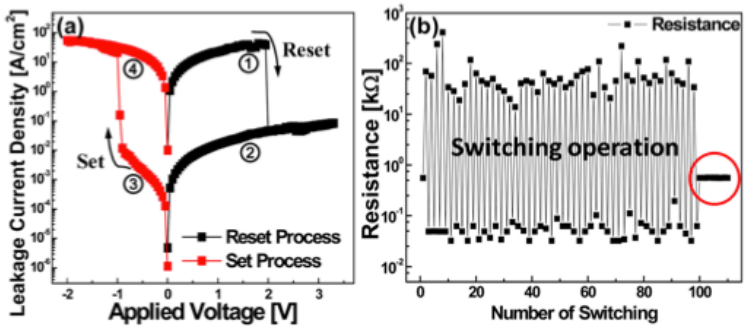

FIG. 1. (Color online) (a) The electrical switching and (b) endurance properties of graphene oxide RRAM consisted of Al/GO(30 nm thickness)/ITO structure.

Figure 4: Current against sweeping voltage for a bipolar switching mechanism in an Al/GO/ITO device, and switching endurance, extracted from the article of Hong et al. [6]

The effect of bottom contacts was also quite important. Indeed if the roughness is too high, the GO layer had such cracks and rough surface, that the top electrode material could easily penetrate and then build filaments which hindered the switching operations. This drastically reduced the device lifetime (only 100 cycles) because of the formation of a definitive conductive path between the two electrodes. These results have been pointed out by X-ray photoelectron spectroscopy (i.d. XPS) measurements that pointed out the permanent presence of Al near the bottom electrode as the main raison for failure. Figure 5, extracted from Hong's article, shows these XPS results.

In order to avoid the failure mechanism linked to the formation of permanent conductive filaments through the material cracks, one suggestion is to use deposition techniques which allow a more uniform distribution of the deposited material. The spraying machine allows the deposition by spraying the graphene oxide while heating the substrate to avoid the coffee ring effect which is responsible of the non-uniformity of the deposition. The coffee ring effect is the pattern left by a puddle of particle-laden liquid after it evaporates. This uniform deposition allows preventing the formation of cracks linked to the roughness in the GO layers.

We can also notice that the graphene oxide-based resistive memories fabricated and tested in other works were found to work under a bipolar switching mechanism [4] [12]. The tests we have carried out and discussed in chapter III also had that characteristic. But there were also works finding unipolar mechanism [13].

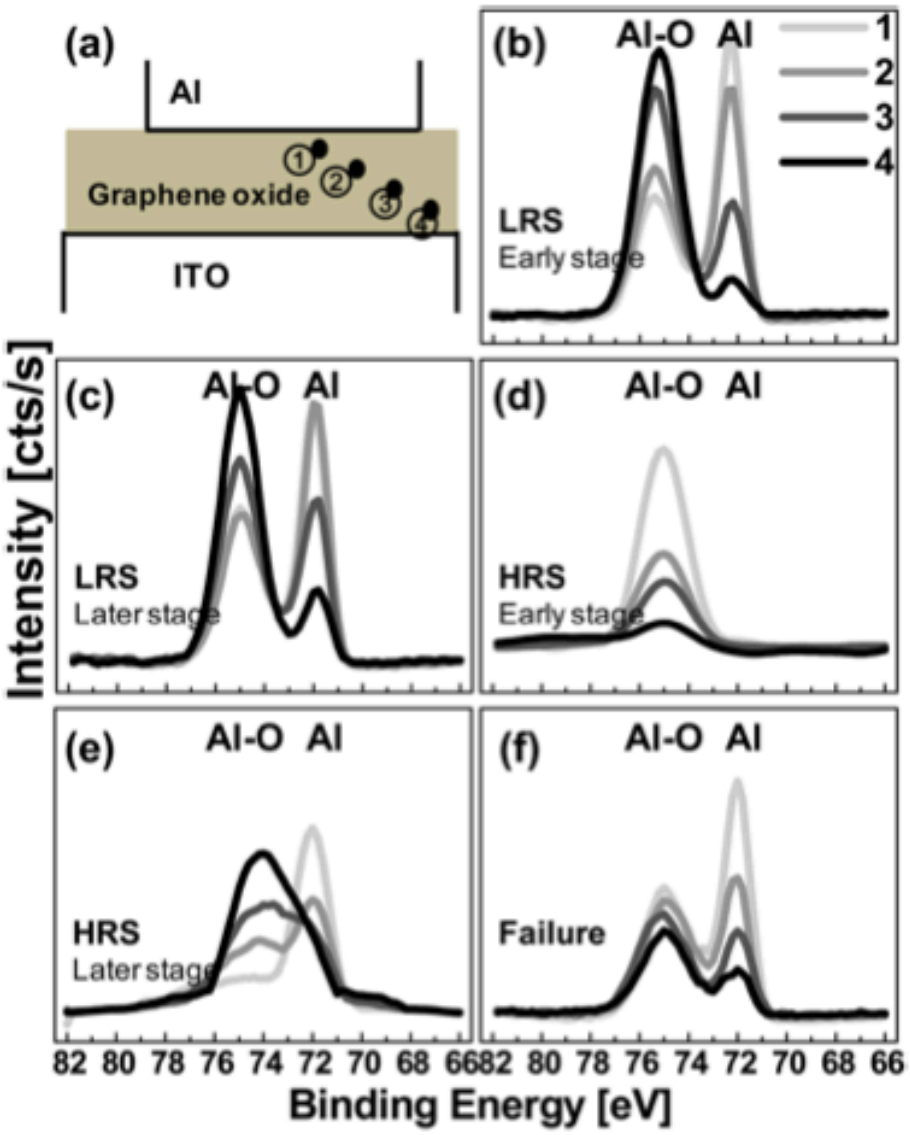

FIG. 5. (Color online) The Al depth profiles were analyzed for the same five samples used in Fig. 4. (a) XPS analysis points; (b) LRS for early stage; (c) LRS for later stage; (d) HRS for early stage; (e) HRS for later stage; (f) failure state.

Figure 5 : *XPS analysis of the eventual top contact diffusion into the graphene oxide layer, preventing the switch mechanism*

Chapter 2

Device fabrication

Our goal has been to *fabricate M-I-M structures (cf figure 1)*. The samples we have started with, were simple p-doped-Si two inches wide, 250 µm thick wafers, on which has been deposited a 40 nm platinum thin film (with a 5 nm Ti layer between, to favor optimal adherence) by the team responsible for the *evaporation technique* in the laboratory. These wafers were two inches, we cleaved them to get samples about 1 square centimeter each.

Figure 6 : *Simple layout of a p-doped silicon wafer, with a 40 nm Pt coating*

On these structures I was responsible for the next steps of the fabrication : a graphene oxide thin film was deposited thanks to a new, innovative method : *spraying*. Then the device went through the *photolithography and lift-off phases*, before being *tested electrically*.

2.1 Spraying deposition technique

2.1.1 The spraying machine

The work of spraying a graphene oxide thin film was achieved using a recent deposition technique, patented in France in 2010 by one of my supervisors in Palaiseau among others, and called "Method for depositing nanoparticles on a surface and corresponding nanoparticle depositing appliance" [8].

We have used this method for depositing nanoparticles on a surface to form a thin film of graphene oxide. A suspension of nanoparticles in solution in a liquid, in our case graphene oxide flakes diluted in water, has been sprayed on a sample pinned to a heated plate. The heating allowed a fast evaporation of the solvent, avoiding the coffee ring effect to provide an uniform deposition. The heated plate was moved by a robot which controls its horizontal translations and the vertical translation of the spray valve. The choice of moving in the horizontal plane the heated plate can be explained by the fact that vibrations are created when transmitting the motion. The impact zone of the spray was moved while the spray remained fixed and thus by programming the movement of the heated plate, we could set a path for the spraying on a sample pinned on the heated plate. The spraying is dynamic and with an optimized sweeping of the heated plate. Figure 7, 8 and 9 represent the spraying set-up and the spraying valve.

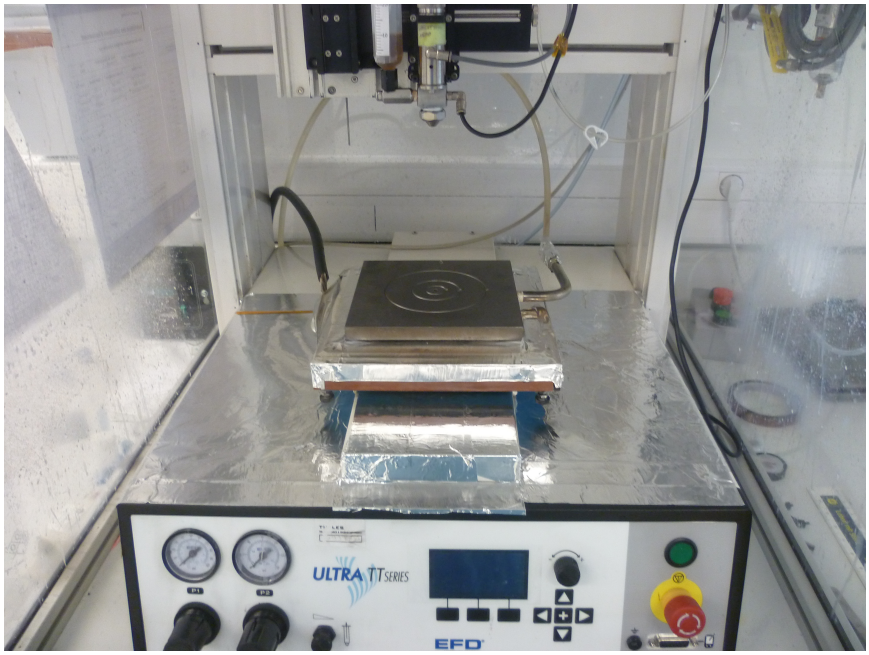

Figure 7 : *Spraying set-up*

Figure 8 : *Spraying valve*

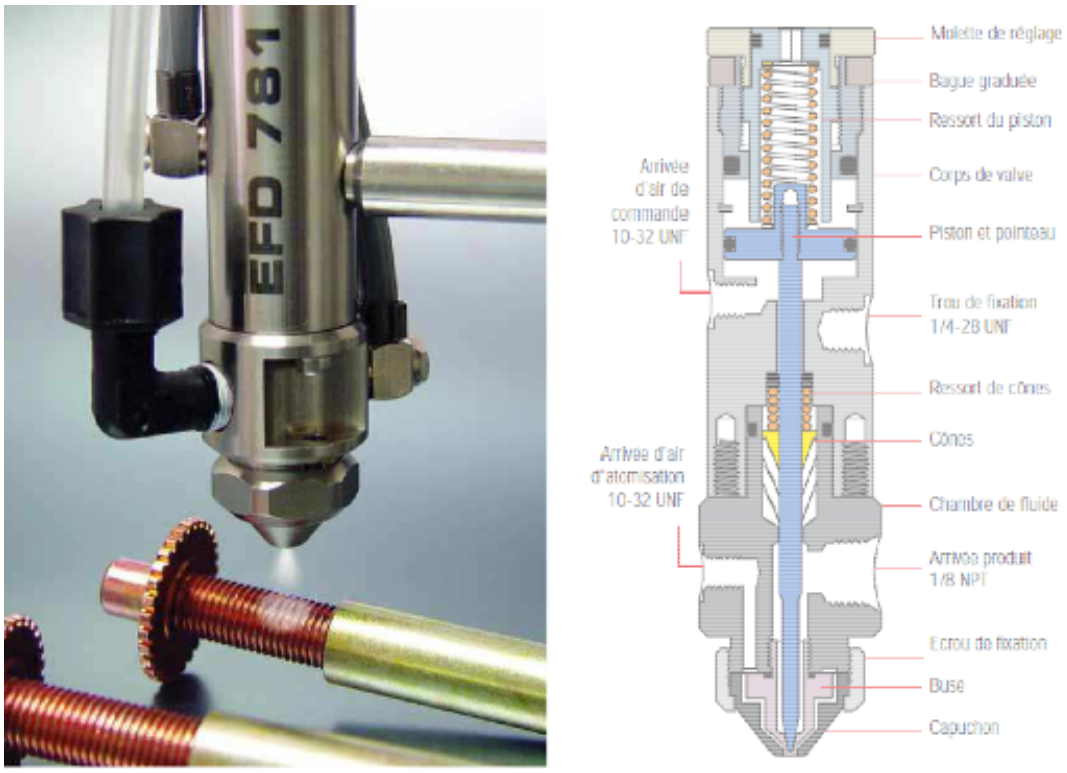

Figure 9 : *Spraying valve used for the spraying (Nordson EFD 781 spray valve)*

2.1.2 The spray control parameters

At this step, the samples consisted in p-doped-Si semiconductor two-inches wafers, on which a 40 nm platinum thin film had been grown by evaporation technique. We had different parameters to optimize the deposition of the graphene oxide.

The spraying has been carried out according to a coil-shaped pattern (see figure 10). The process of fabricating a thickness-controlled uniform thin film of graphene oxide depends on the three following parameter groups :

1. The temperature of the heated plate
2. The opening of the spray valve / The spraying distance between the spray valve and the heated plate / The lateral distance Δ between two successive sprayings within the spraying pattern
3. The number of iterations of the spray program / The concentration of GO in the solvent (in our case, solvent is water)

Regarding the first parameter, we started the experiments choosing the values commonly used for a previous similar process : the fabrication of supercapacitor electrodes based on mixtures of graphite and carbon nanotubes [10].
The deposition temperature has been set to 140°C, value which has been efficient for supercapacitor fabrication. We later set the temperature at 170 °C, considering that we have worked on thinner films compared to the ones of supercapacitors (for which they were 20 µm thick). We also needed a more uniform surface, which the temperature allows, since it is an important parameter to avoid the coffee ring effect.

A previous Ph.D. student, Louis Gorintin, working at Thales/CNRS has carried out a study to understand better the spraying [9]. He wanted to ensure the machine could spray a uniform enough thin film. He identified *three parameters having effect on the uniformity of the spraying* : the opening of the spray valve, the spraying distance between the spray valve and the heated plate, and the width between two longitudinal successive spraying (parameter group number 2).

He had first to look at the spatial distribution of the droplets' deposition on the substrates, which is a function of the spraying distance. The observed spraying is circular, has its intensity from the center of the spraying described by a gaussian function, and its diameter varies depending on the distance between the substrate and the nozzle of the spray gun. There is also to determine the opening of the nozzle of the spray gun. When this is done, we obtain the width of the gaussian spray in function of the height of the spraying. The deposition being gaussian in case of a static spray, it's not possible to obtain a uniform deposition in this case. Since we want an uniform deposition, the spraying has to be dynamic and with an optimized sweeping of the heated plate. For this we used a programmable robot with 3 axes of motion.
Hence the spraying pattern had already been determined. Figure 10 displays this pattern. Distance L was 2 cm, Δ was 5 mm, and the vertical distance between the heated plate and the spraying valve was 12 cm.

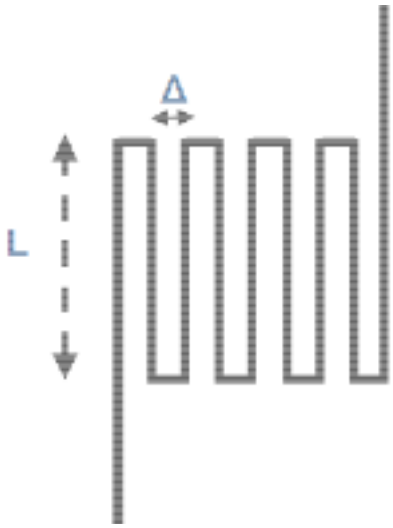

Figure 10 : *Spraying coil-shaped pattern, L was fixed to be a little higher than our sample, Δ was determined according the spray flux shape and was set to 5 mm*

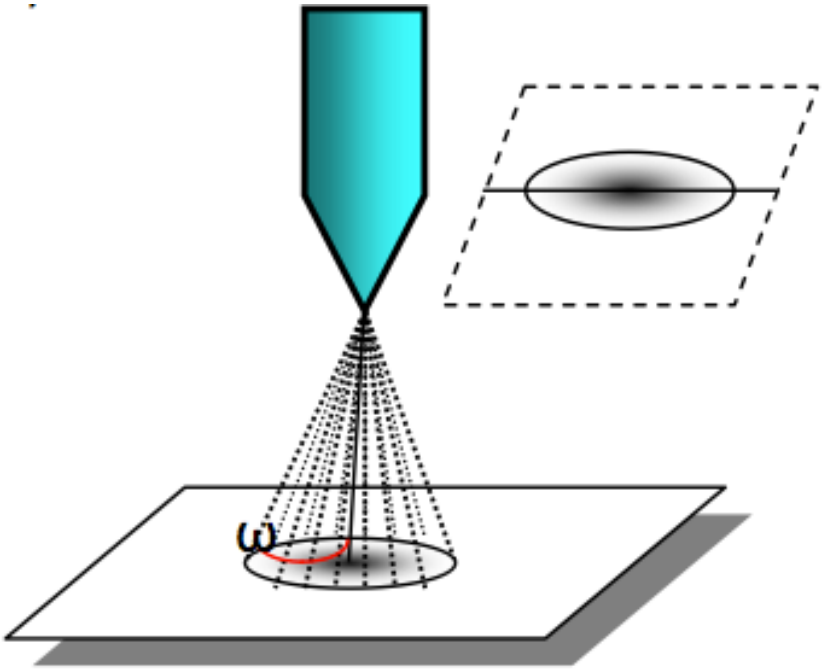

Figure 11 : *Simple representation of the distribution of the droplets' deposition on the substrates*

Thus remained the third group of parameters : number of iterations of the spraying program, concentration of graphene oxide in the solvent.
We could have considered to check the speed of the spray gun on which also depends the thickness of the deposited layer. But the speed was directly connected to the number of times the machine's deposition program was repeated. Indeed repeating for example five times the same program at a speed five times slower is equivalent. Thus, we have fixed the speed of the program and didn't have to consider it further.

The concentration of graphene oxide and the number of iterations of the spraying program were thought to have a linear influence on the film thickness.

We had to ensure that for our use, at this plate temperature and with these uniformity parameters (parameter group 2), we obtained the expected dependence of the film thickness with parameters of the parameter group 3, while getting a satisfying uniformity revealed through the roughness of the sprayed thin film. **For the control of a satisfying roughness, we aim at a (roughness / deposited film thickness) ratio under 15 %.**
This process control is presented in chapter 3 section 1.

Figures 12, 13 and 14 display optical microscope images of a deposited graphene oxide layer on our Si/Pt substrate.

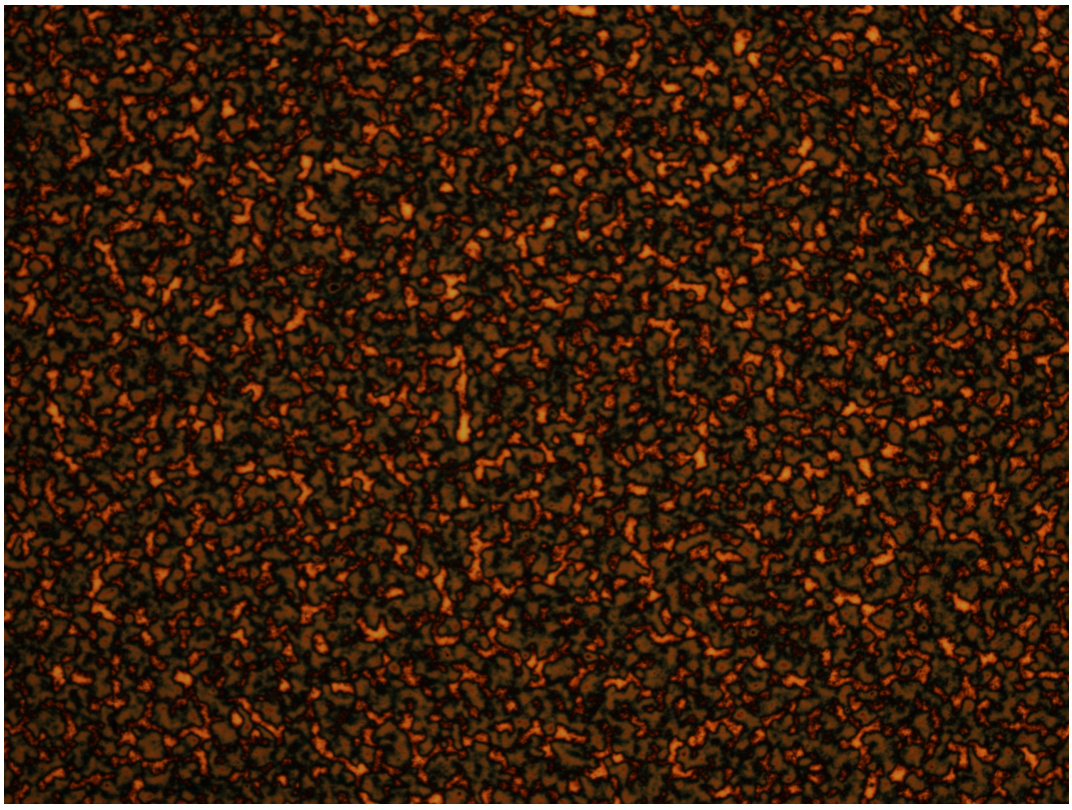

Figure 12 : *Optical image (x5) of a graphene oxide layer deposited on a Pt electrode*

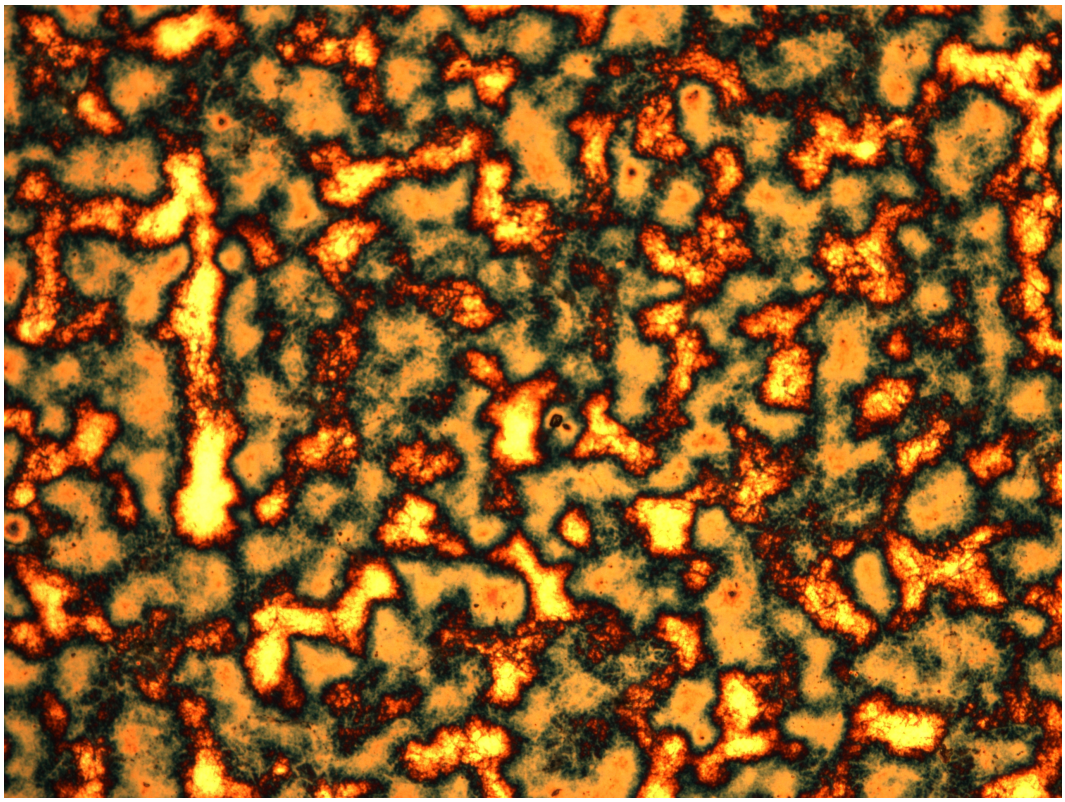

Figure 13 : *Optical image (x20) of a graphene oxide layer deposited on a Pt electrode*

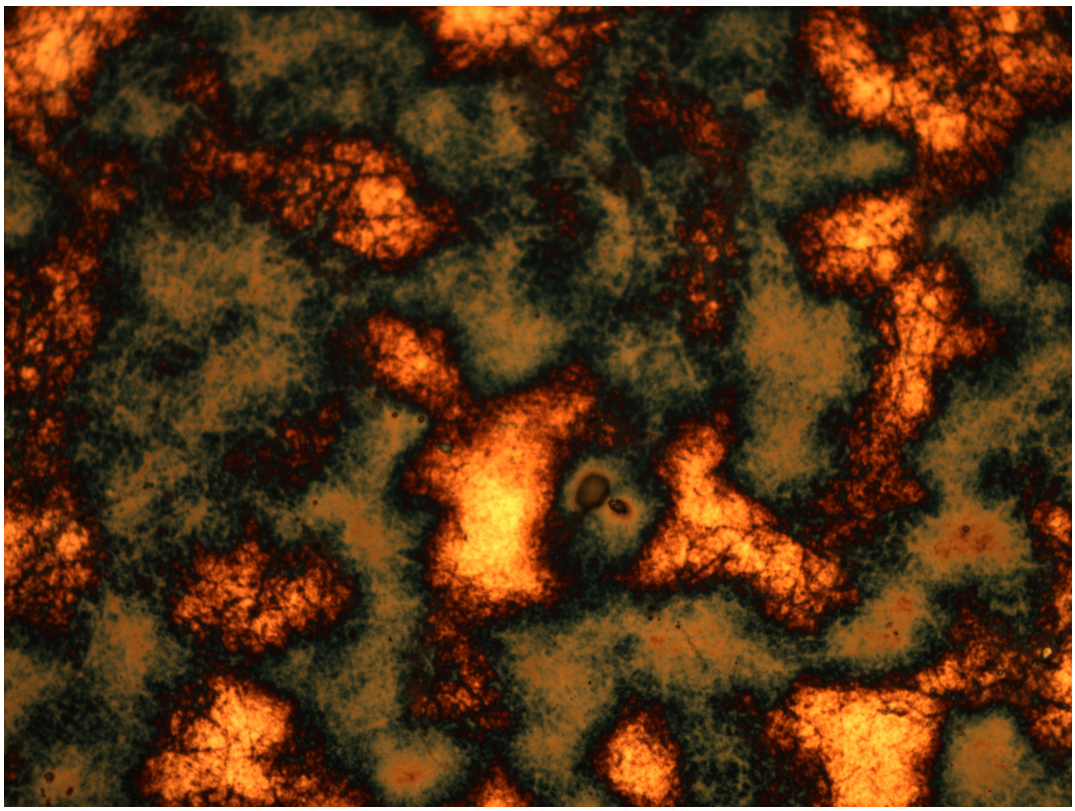

Figure 14 : *Optical image (x50) of a graphene oxide layer deposited on a Pt electrode*

These images led us to think that the roughness of the deposited graphene oxide layer was too high, but after measurement we obtained acceptable values for the root mean square (RMS) value of the roughness (see chapter 3 section 1).

To control our process of graphene oxide deposition, we used a flow-meter based on the Coriolis effect (Bronkhorst Cori-Tech, mini Cori-Flow). Even though this is a cutting-edge type of flow-meter, we had the misfortune that a tube of the flow-meter got full of nanoparticles. Indeed the use of very thin particles caused the blocking of the flow-meter during the internship. We had to send the device to the after-sales service of the fabricant and could not benefit from it.
The aim of the use of such a device was to control the flow of the solution going to the spraying valve to ensure a uniform deposition.
We thus were not able to observe this characteristic, but investigated the uniformity of the spraying by checking the roughness of the deposited graphene layer.

2.2 Photolithography

After the first Pt layer was deposited by evaporation, and the graphene oxide was sprayed, we had to carry out the top electric contacts fabrication. We used the technique of *photolithography* followed by a *deposition (evaporation or sputtering)* performed by the common platform team of the laboratory, and a *lift-off step*. The objective was to create several contacts for the tip that was used for the electric characterizations (the tip had a diameter of 100 µm).

Figure 15 displays an image extracted from a photolithography book [11] that sums up the photolithography process and explains the difference between a positive and a negative resist.

Since it is probably pretty well known to the readers, photolithography technique was not explained in full details in this section but only summarized.

It is a technique used to achieve a pattern with a material we want on a thin film.
The pattern design is in the photolithography mask. We deposited a thin layer of photosensitive resist in a uniform way and made sure it sticked to the surface we wanted to deposit the metal on. We spread the resist on the samples using the spin coating technique. This device allows high-speed rotation of the sample we want to cover with resist, the sample being kept steady by a vacuum suction. The faster the spin coating speed, the thinner the resist layer. We can see on figure 17 that the resist we used, SPR 700 1,2 is 1,2 µm thick when it is spinned at 4000 revolutions per minute (RPM) like we did.

These resists are organic compounds (generally thermoplastic polymers) of which solubility is modified by light exposure. The resists we used are called "positive" (see figure), in the sense that we sent the light through the pattern of the mask to create square areas which were the contacts aftertwards. For a positive resist, light exposure causes a breaking of macromolecules, hence a higher solubility of the exposed areas during interaction with the developer. Indeed the exposed resist is then removed during development in an organic solvent. To perform the optical lithography we used a mask aligner to align the mask with sample.

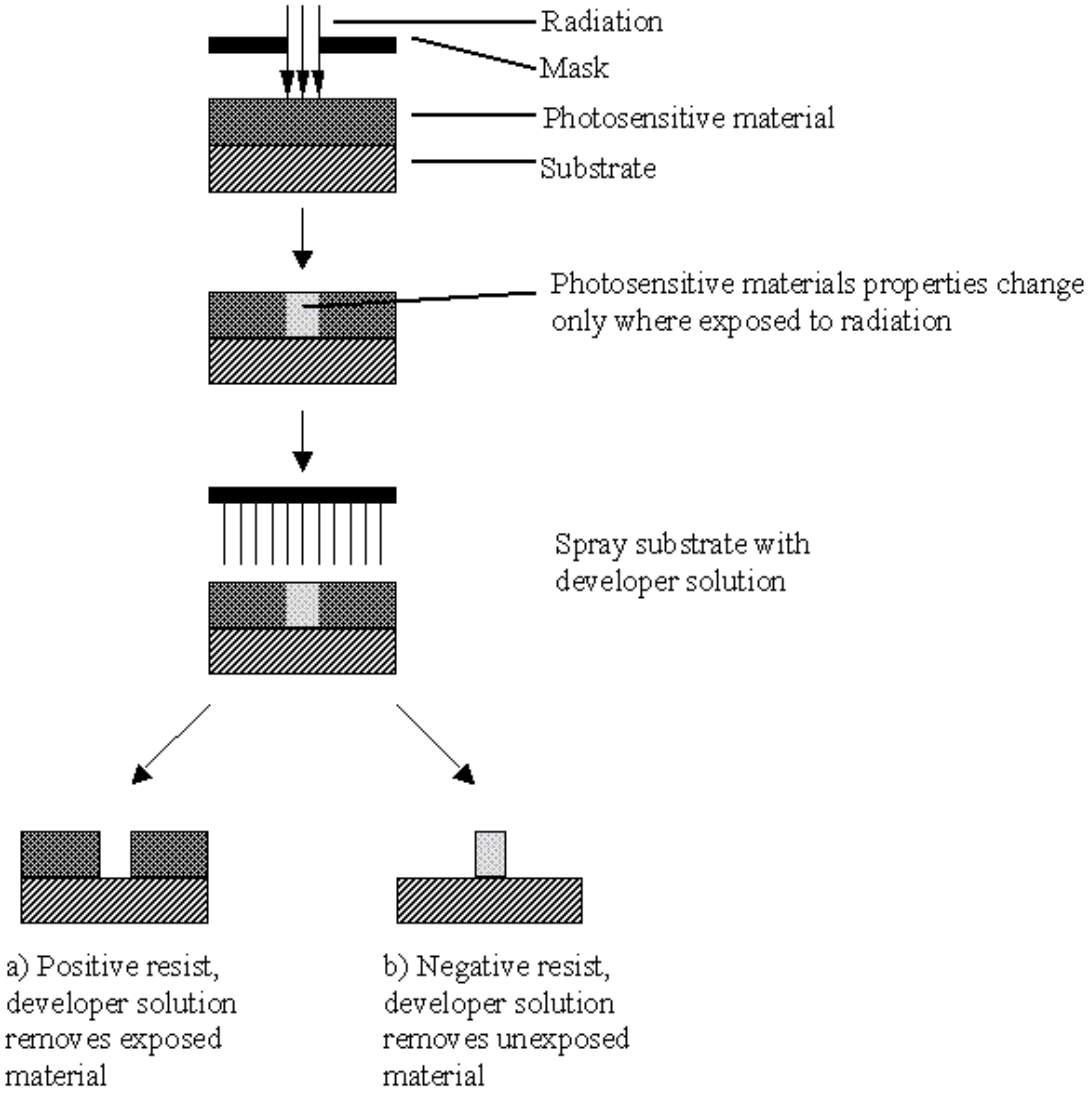

Figure 15 : *brief explanation of the photolithography steps*

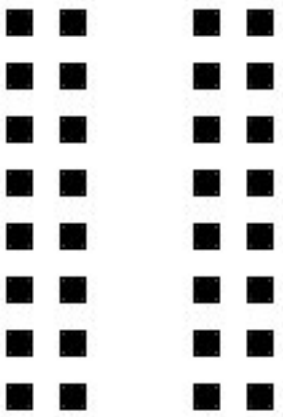

Figure 16 : *Very simple layout of the different square contacts (100 µm wide) we fabricated*
Every sample provided several series of 32 top contacts like the ones represented, to conduct electric characterizations

Finally metal was deposited all over the surface by evaporation or pulsed deposition techniques (this was performed by the shared clean-room platform staff), and we performed a last step of lift-off, that is to say we completely removed the resist leaving on the substrate the metallic nanostructures or the non-etched parts. Sometimes an ultrasound bath was necessary to get rid of the whole resist.

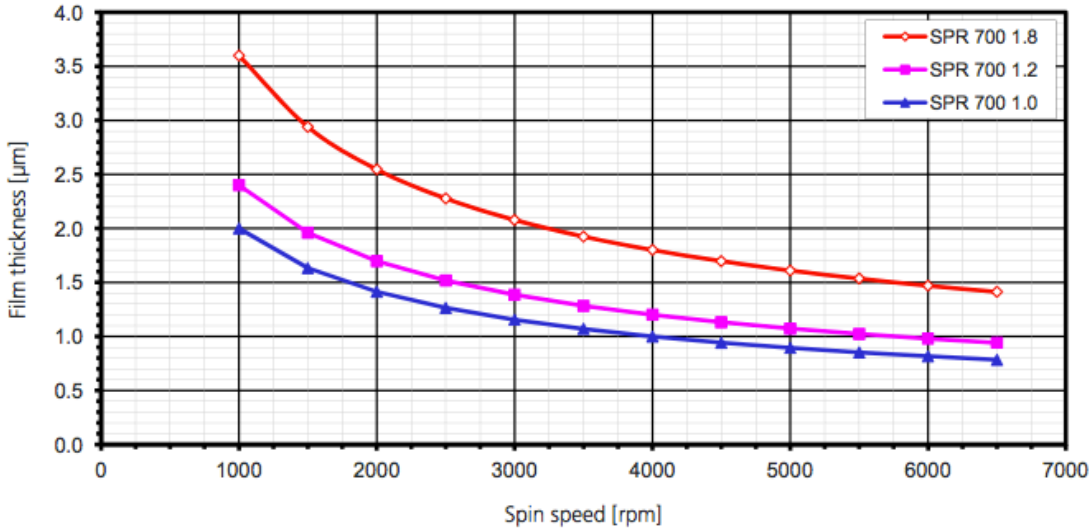

Figure 17 : *Curve representing thickness of the resist layer as a function of the spin coating speed. The resist we used was SPR 700 1.2*

The protocol of the steps we performed during photolithography is the following :

1. Substrate cleaning with acetone and drying with nitrogen
2. Soft bake to remove the eventual imperfections (95°C for 30 s)
3. Spin coating (4000 RPM for 30 s) of the resist (SPR 700 1.2 micron)
4. Annealing of the sample on a heated plate at 95°C for 60 s
5. Exposure with positive mask at broadband light
6. Annealing of the sample on a heated plate at 115°C for 60 s
7. Development: 30 s in developer (MFCD26, Microposit)
8. Substrate cleaning with acetone and drying with nitrogen
9. Metallization (evaporation or sputtering) : thickness around 100 – 200 nm
10. Lift-Off
11. Eventually ultrasound bath

Figure 18, 19 and 20 display optical microscope images (x20) of Cu top electrodes that were created above graphene oxide.

What we can see on figure 20 is a graphene oxide layer covered with resist. The squares are the areas where there was light exposure, thus are the areas where there didn't remain resist after development.

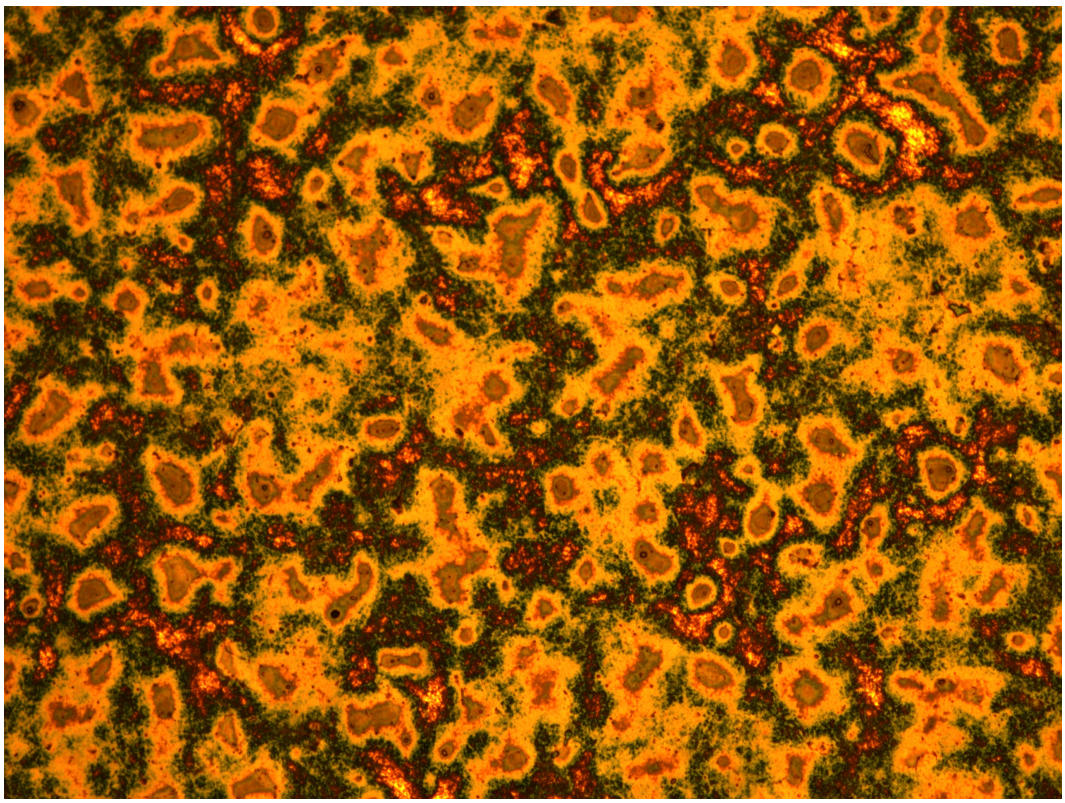

Figure 18 : *Optical microscope image (x50) of a graphene oxide layer before depositing the resist*

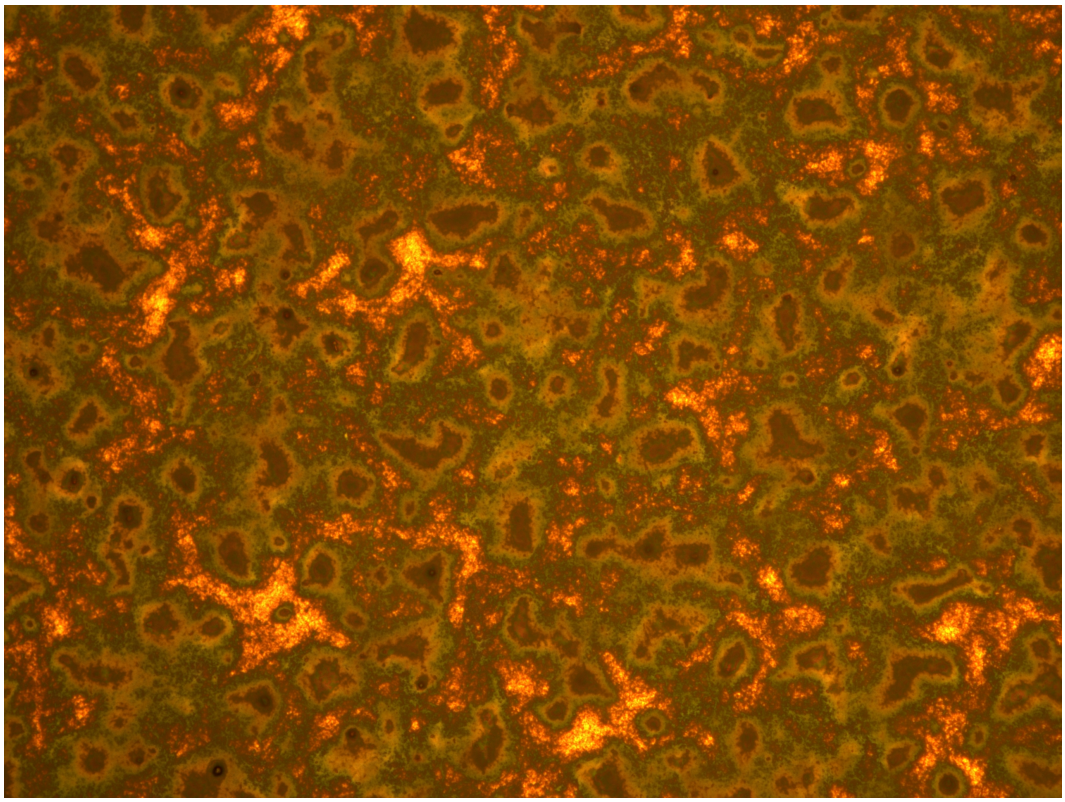

Figure 19 : *Optical microscope image (x50) of a GO layer after depositing the resist*

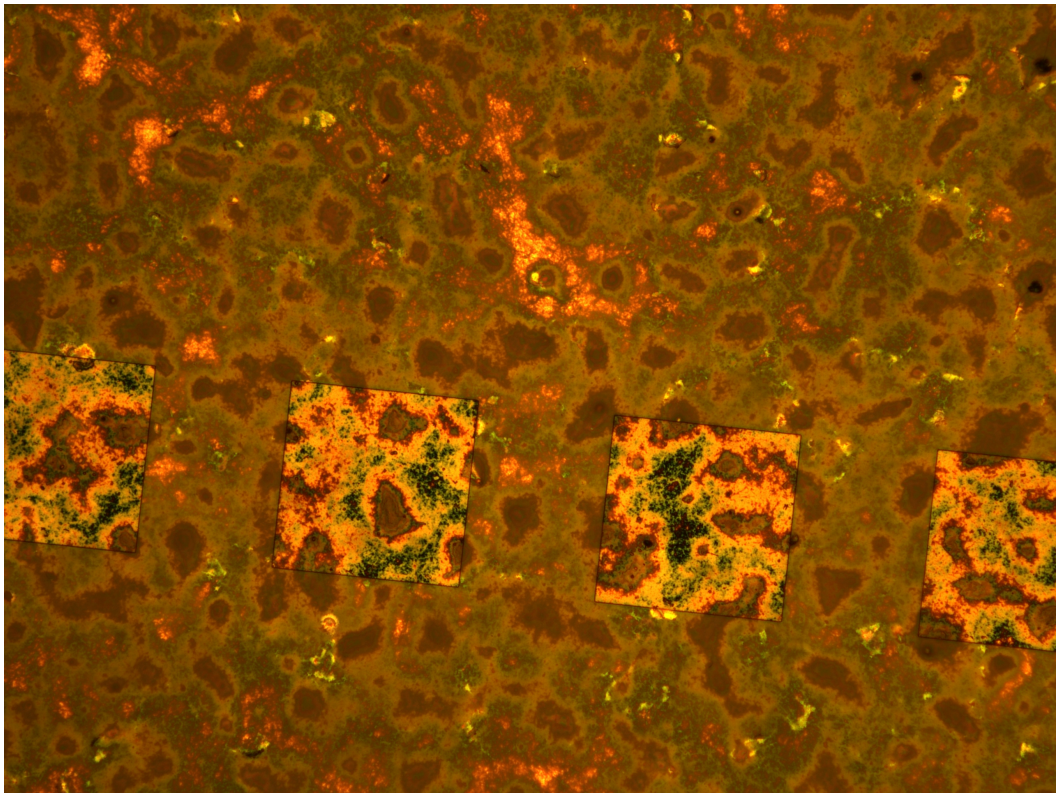

Figure 20: *Optical microscope image (x50) of a GO layer after developing the resist*

Chapter 3

Experimental results

This chapter displays the obtained experimental results.
In the first section, the control of the spraying process is presented. After this step the samples go through photolithography, deposition and lift-off, see chapter 2 section 2.
After the lift-off the devices are tested by electric characterizations, the second section of this chapter is the analysis of such electric characterizations.

3.1 Control of the spraying process

After the graphene oxide coatings were deposited, we needed to have a way to control the width of the layer, and its roughness as well.
As we've seen before in the work of S.K. Hong in which the Korean team investigated the role of the bottom electrode [6], roughness is important since we need to have a good interaction between the bottom-electrode and the graphene oxide layer. Indeed a low graphene oxide roughness as well as the lack of cracks in the GO layer, prevent the bottom electrode from penetrating easily in the GO layer, which would allow the creation of conductive metallic filaments and thus would make the switching mechanism undetectable. The article made a study and proved the correlation between the bottom-electrode/GO interaction (which depends on the bottom-electrode material) and the getting of a switching mechanism or not.

As mentioned earlier in chapter 2 section 1, our goal was to ensure that for our use, at fixed plate temperature and with these uniformity parameters (parameter group 2 : L, Δ and the spray vertical distance), we could establish a process to obtain as an output the thickness of the deposited graphene oxide layer depending linearly on the above mentioned parameter group 3 : number of iterations of the spray program / concentration of GO in solution. This process has also to maintain a satisfying roughness.

So we decided to investigate parameter group 3 to determine if at fixed temperature and uniformity parameter group 2, we are able to control the process linearly, maintaining a satisfying roughness.

To carry on this investigation, we used an atomic force microscope (AFM) and a profilometer.
Six samples were examined on which we tried different graphene oxide concentrations and different number of program iterations for the process (see table 1).

AFM is a scanning probe microscopy technique which allows to provide topographical maps of the sample surface with sub-nanometric resolution. We used the contact mode of the AFM to scratch the graphene oxide deposited layer. Then we used the tapping mode to determine the height between the scratched area and the non-scratched one, leading us to the graphene oxide thickness. Each reading of the height was carried out two or three times. The AFM image used to determine the height of the first sample (sample A) can be found in the **Appendix**. On this image, the height difference is read with the blue or red crosses. We then calculated the average of these measurements, and the error bars representing the standard error. Another AFM image also displayed in the Appendix allowed us to determine the roughness of the graphene oxide film. The scratching causing a displacement of the material in the scratched area, there was a border delimiting the different areas.
Profilometer measurements of the thickness to check the agreement of the results were performed by the staff of the shared clean room of the laboratory. They scratched the surface of the samples with a toothpick, and then determined the thickness of the layer.

We obtained the following results : see table 1.

Sample	N° of program iterations	GO conc° (g/L)	Thickness (nm) AFM meas.	Std error (nm) AFM meas.	Roughness (nm) AFM meas.	Thickness (nm) Profilom. meas.
A	16	0,25	75	8	11,2	70
A'	20	0,25	99,5	37	13,7	100
A''	48	0,25	253	54	9,42	250
B	16	0,2	77	23	21,8	70
B'	16	0,25	105	6	14,9	100
B''	16	0,4	155,5	43	20,1	150

Table 1 : *Black : Identification of the different samples tested, by number of program iterations and graphene oxide concentration (g/L).*
Blue : Graphene oxide thickness obtained by AFM measurements, standard errors of these measurements, roughness (Root Mean Square value)
Green : Graphene oxide thickness obtained by profilometer measurements

We then wanted to determine the roughness / thickness ratio to have a feedback on the uniformity of our deposition. The results are displayed in table 2.

Sample	Thickness (nm) AFM meas.	RMS roughness (nm) AFM meas.	Roughness / Thickness (%)
A	75 nm	11,2 nm	14,9
A'	99,5 nm	13,7 nm	13,8
A''	253 nm	9,42 nm	3,7
B	77 nm	21,8 nm	28,3
B'	105 nm	14,9 nm	14,2
B''	155,5 nm	20,1 nm	12,9
	Average roughness/thickness (%)		14,6

Table 2 : *Roughness / thickness ratio for all six samples, average of this ratio*

The average roughness / thickness ratio was 14,6 %, which is under 15 % and is commonly considered as **satisfying** for further processing.

To check the linear dependence of the graphene oxide thickness, we drew the results contained in table 1. See figures 21 and 22.

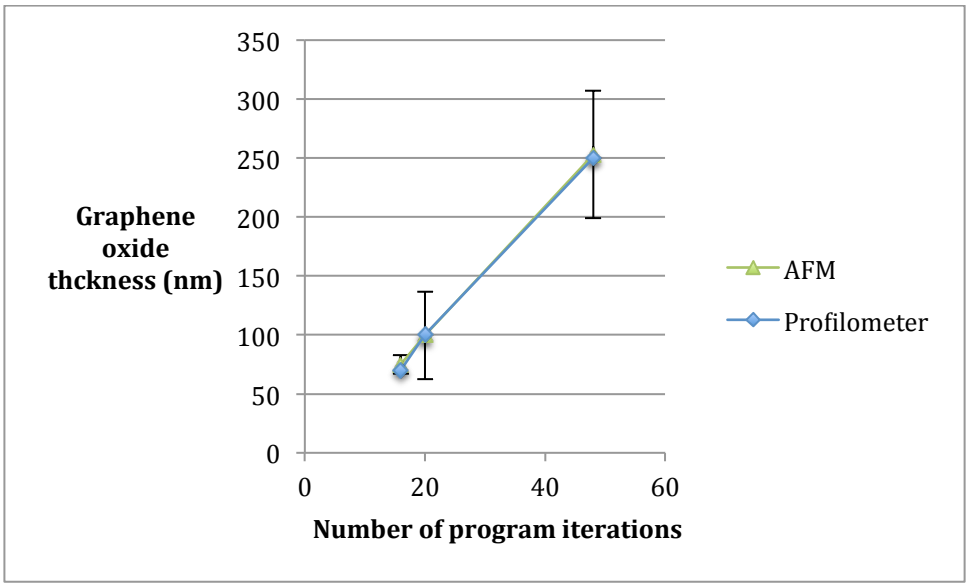

Figure 21 : *Graphene oxide thickness against number of program iterations, results obtained with AFM and profilometer measurements. The error bars are for the AFM measurements*

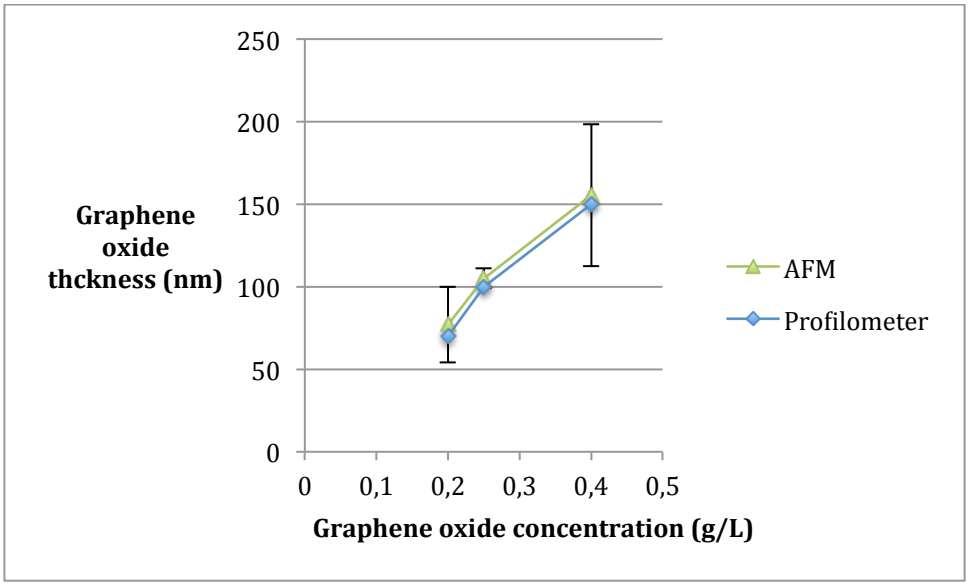

Figure 22: *Graphene oxide thickness against graphene oxide concentration, results obtained with AFM and profilometer measurements. The error bars are for the AFM measurements*

Even though the measurements could be improved by increasing the number of measurements for each layer thickness, from figure 21, we can see that we have a linear correlation between graphene oxide thickness and the number of program iterations.
With a fast calculation, we can see that these two curves allow us to conclude that in the average, every program iteration deposits a thickness of about 5 nm on the surface. This is an approximate estimation, which only serves the purpose of giving the reader an estimation of the deposited thickness by program iteration.

Similarly, from figure 22, we can conclude that there is also a linear correlation between the thickness and the graphene oxide concentration.

3.2 Electric characterizations

For the reader's comfort, we reproduce figure 1 on the next page, so as to remind them the structure of the devices fabricated.

The following part consisted in testing the fabricated devices, to see if those presented a switching mechanism. This phenomenon is complex and still unknown on many points, and we were trying to recognize patterns already observed and understood.
We were lucky enough to find different understandable behaviours in response to the experiments we carried out. These were current measurements during voltage sweeping experiments.

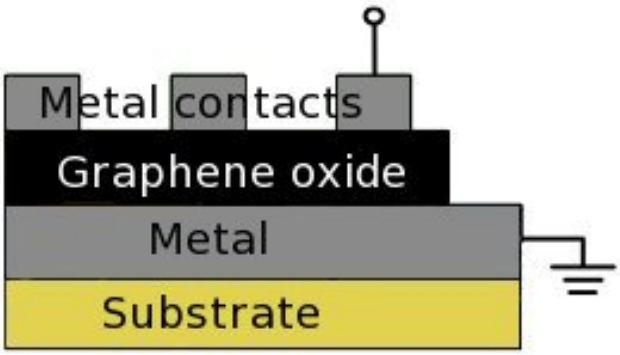

Figure 1 : *Metal-Insulator-Metal structure for a RRAM memory*
Here : insulator material is graphene oxide like in the devices we fabricated

In order to improve the measurement time, it was necessary to build a LabVIEW program which allows the user to carry out I-V measurements without having to make each measurement by hand dicontinuously. Our aim is to be able, depending on the context, to adjust the characteristics of the voltage and to measure the current thanks to a probe measurement and Keithley SourceMeters. So as to accomplish these measurements, we decided to use the sweep mode of the voltage source which fixes the extreme values of the voltage that we want to vary and the measurement step among other parameters.

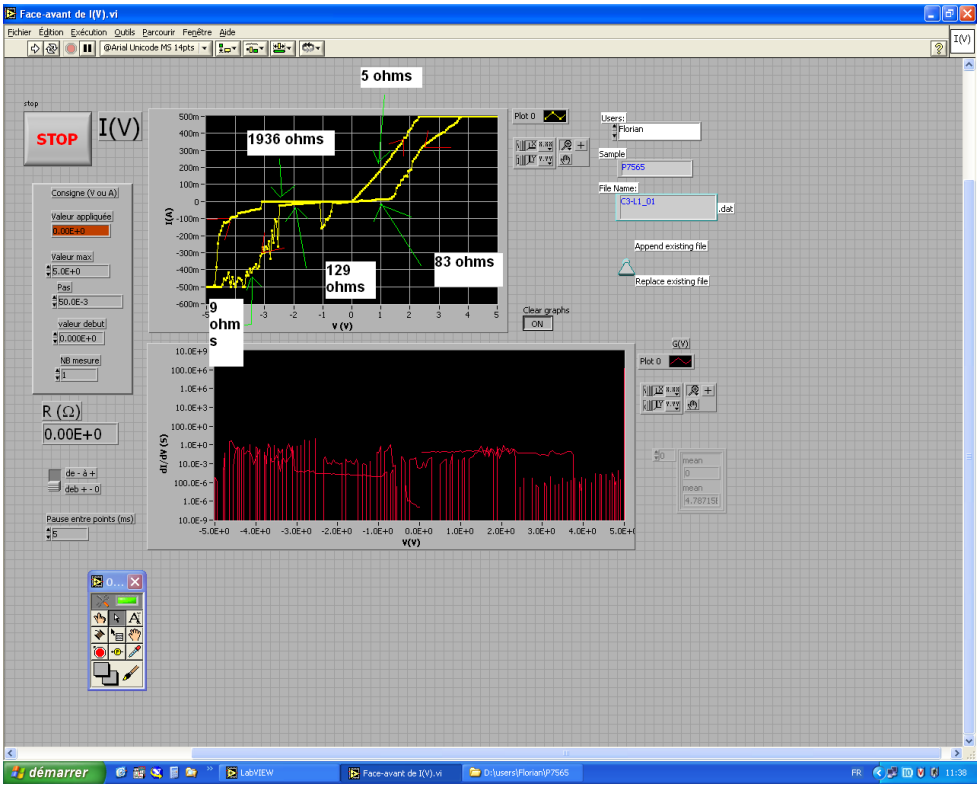

Figure 23 : *Screenshot of the LabView program used to make the measurements*

3.2.1 The "resistance reading" test

Table 3 displays the tested samples that were acceptable after fabrication. It classifies them according to the two chosen variables that were set during the photolithography / metallization / lift-off steps of the process :

- the top-electrode material
- the thickness of this top-electrode

Among these two variables, the top-electrode material is very important since, as was presented in chapter 1 section 2 subsection 2, Hong et al. [6] had obtained switching mechanisms only with electrochemically active electrodes.

We decided to test this factor and chose four top-electrode different materials : two electrochemically active (an alloy of AlCu, and Cu), and two electrochemically inert (Au and Pt).

On these devices, the first test we tried was the « resistance reading » test, since it was a low voltage test (maximum amplitude of the sweeping voltage : 0,1 V). It was a simple voltage sweep from 0 V to 0,1 V, then from 0,1 V to -0,1 V, and back to 0 V.

We repeated this step on every contact fabricated, as a first step to see if it was worth testing further or not.
Indeed after the first tests, we noticed that we obtained low values of resistance for the Au and Pt top-electrode samples (see figure 25). On the contrary we had high resistance state for some top contacts of AlCu and Cu samples (see figure 24).
Later tests never resulted in a switching mechanism starting from low resistance state to high resistance state and back to low resistance state. Since such switching mechanisms have been observed in graphene oxide based RRAM [6], this could be for two reasons : either the devices fabrication were flawed (short-circuited), or it confirmed the result of Hong et al about the electrochemical nature of the top-electrode.

Sample ID	Top electrode Material	Thickness (nm)	Initial high resistance ?
A	Au	150	No
B	Pt	100	No
C	Cu	100	Yes
D	AlCu	100	Yes
E	AlCu	130	Yes
F	AlCu	200	Yes

Table 3 : *Initial resistance according to the samples*

Despite the low number of measurements and the fact that the photolithography step was not controlled, the results we obtained confirm Hong et al.'s result on the necessity of having an electrochemically active electrode to get a switching mechanism. At the attention of the person who will continue the project, I want to say that it could an interesting lead of investigation continuing to verify this result.

The high values of resistance we obtained suggest that the fabricated devices were OFF and that we were in the case that we had to form a conductive path in the graphene oxide layer.
So the result of the fabrication process which could be used for the rest of the switching mechanism investigation were the M-I-M structures in a high resistance state. For the samples which gave more electric contacts, AlCu 100 nm and AlCu 130 nm, we drew a histogram of the initial resistance (see figures 26, 27).

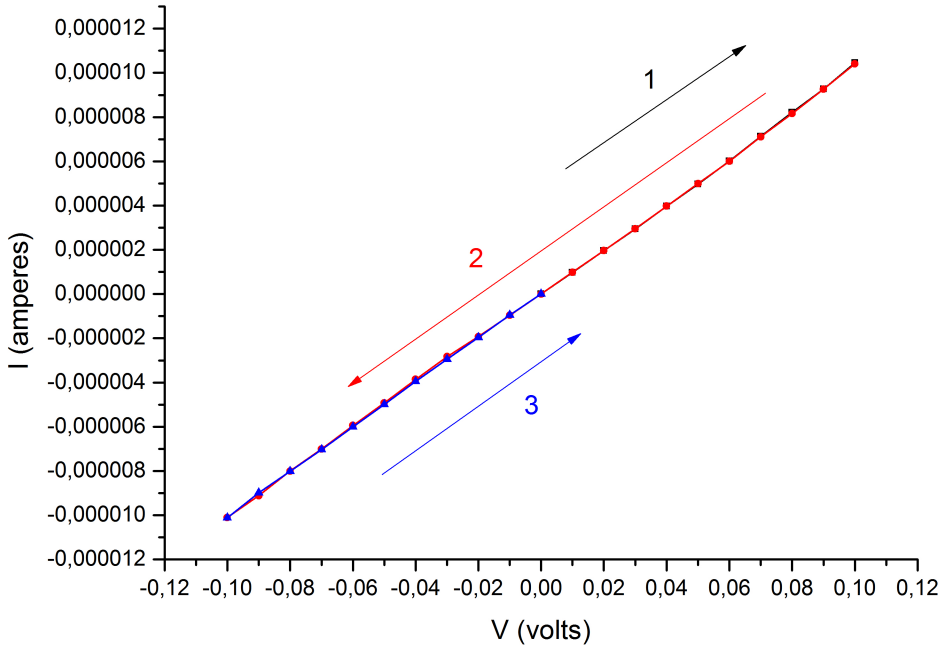

Figure 24 : *Current induced against sweeping voltage for « resistance reading » test for AlCu 130 nm sample (high resistance value : R is around 10 000 ohms)*

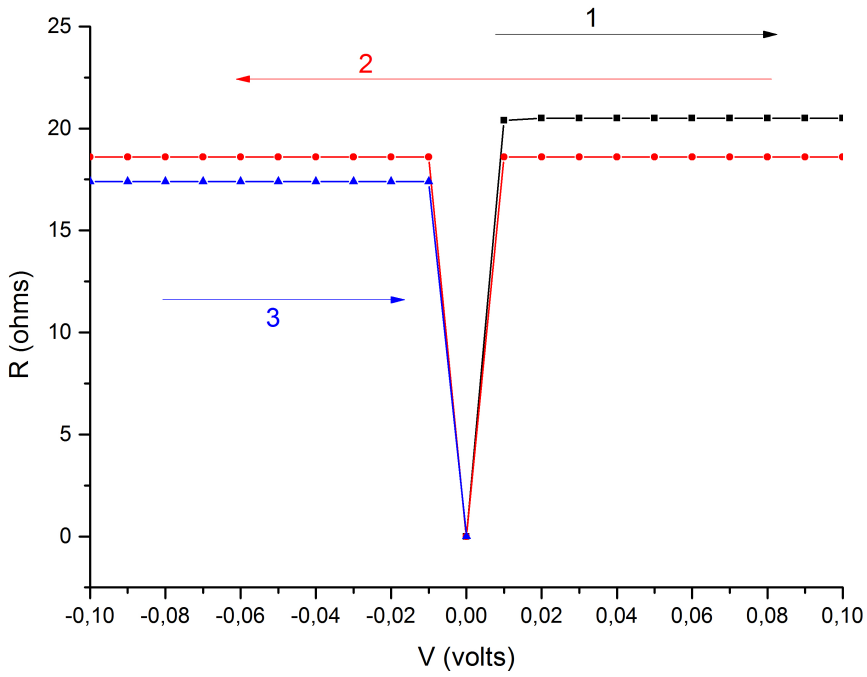

Figure 25: *Resistance of the device against sweeping voltage for « resistance reading » test for Au 150 nm sample (low resistance value)*

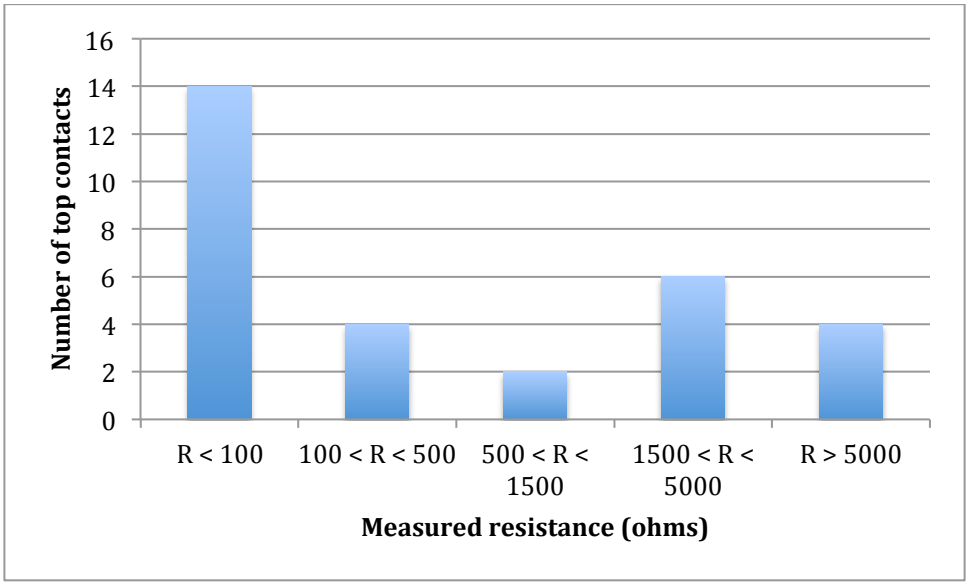

Figure 26: *Measured resistance histogram of AlCu 100 nm top contacts*

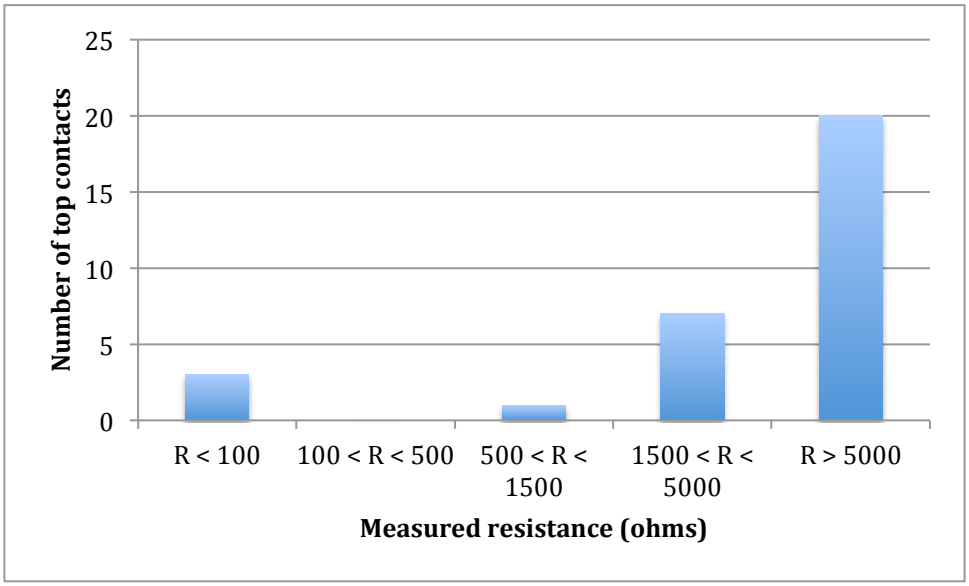

Figure 27: *Measured resistance histogram of AlCu 130 nm top contacts*

We can observe that we obtained a much better yield of tested top-contacts resulting in a high resistance state (i.e. on which we can go on with looking for a switching mechanism).

We set the minimum resistance to carry on further experiments as 500 ohms, we obtained the yields of top contacts further tested :

AlCu 100 nm : 12 / 30 = **40 %**
AlCu 130 nm : 28 / 31 = **90 %**

Thus we obtained a better yield for the thicker top contact, probably because it makes the device more resistant to the contact with the tip of the testing machine.

3.2.2 Further investigation of the switching mechanisms

After the first step of testing, among the different samples which were used for electric characterizations, the following showed to be more interesting and will be discussed later in this part :

- AlCu top-electrode, thickness : 130 nm
- Cu top-electrode, thickness : 100 nm

We tested the top contacts of these samples in a more thorough way, increasing the amplitude of the maximum of the sweeping voltage little by little until we found a significative change in the resistance of the device (switch).
It led us to reach voltages typically around 1,0 - 1,5 V. Higher voltages were proven but they made the device undergo a breakdown, leading to a short-circuit (see figure 28).

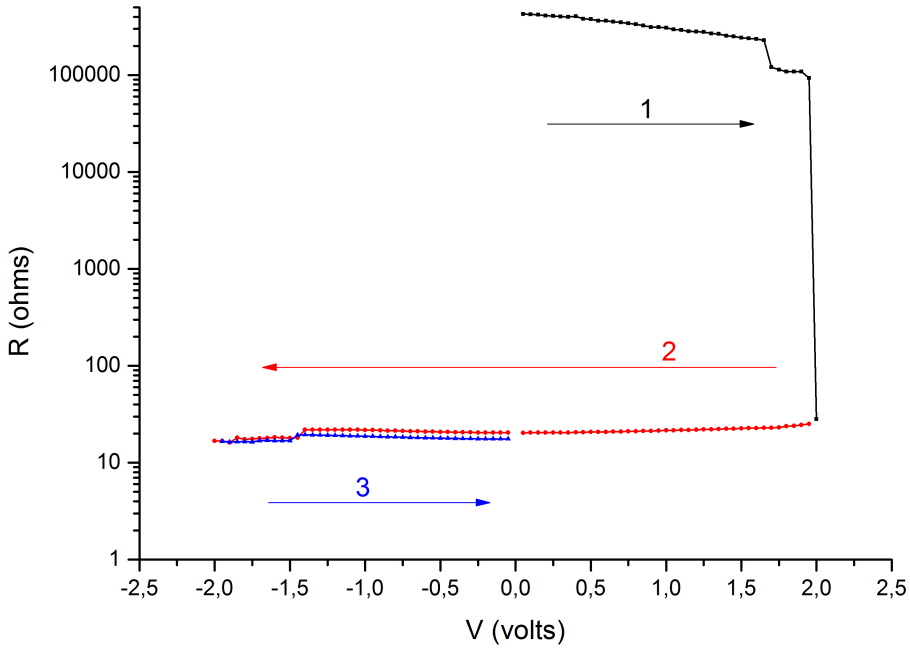

Figure 28: *Resistance of the device against sweeping voltage for the AlCu 130 nm sample. Breakdown of the memory device*

These two devices showed bipolar resistive switching (see figures 29, 30 and 31).

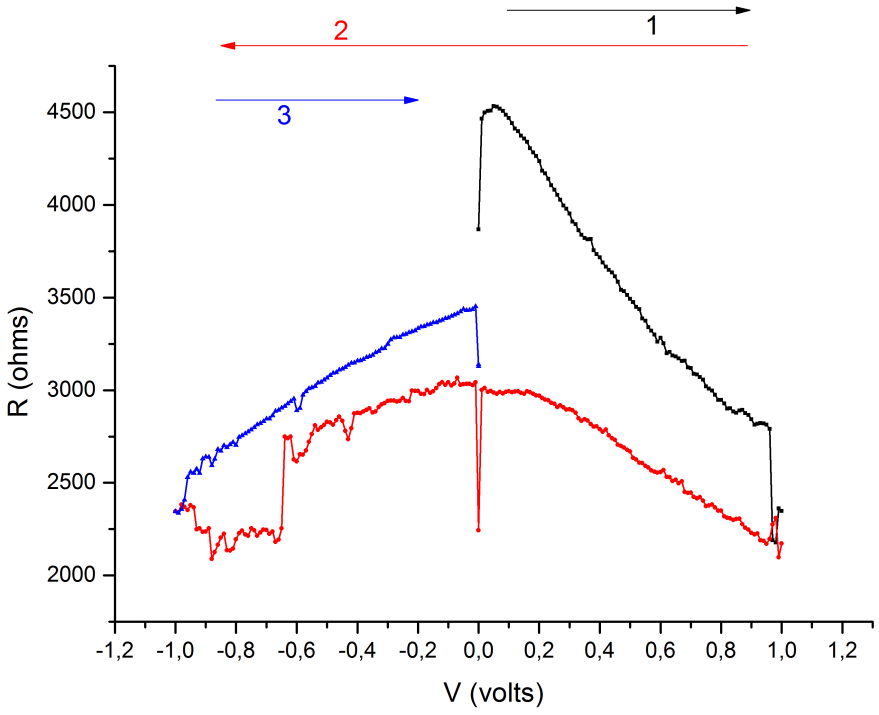

Figure 29: *Resistance of the device against sweeping voltage for the Cu 100 nm sample*

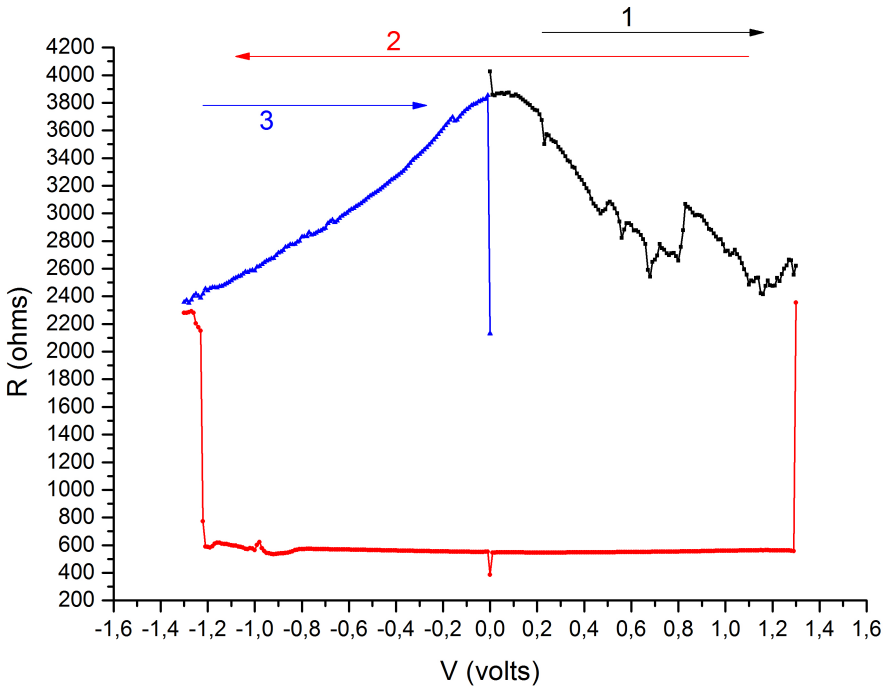

Figure 30 : *Resistance of the device against sweeping voltage for the AlCu 130 nm device. Here we can see a bipolar switching mechanism from a high-resistance state (OFF state) to a low-resistance state (ON) and back to a high-resistance state (OFF)*

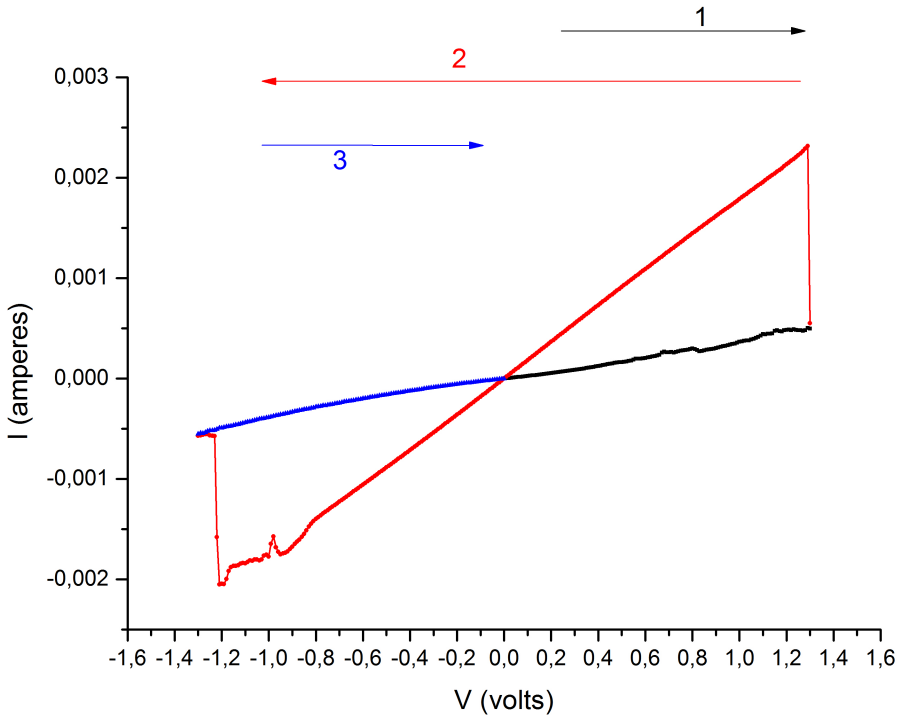

Figure 31: *Current induced againt sweeping voltage for the bipolar switching mechanism for the AlCu 130 nm (different representation but same test as in figure 30)*

There are differences in the switching mechanism found for Cu 100 nm and AlCu 130 nm samples. The switching voltage is higher for AlCu 130 nm : around 1,3 V, for around 1,0 V for Cu 100 nm.
There is to say also, that the switching mechanisms of Cu 100 nm top contacts were less « convincing » than the ones of AlCu 130 nm. Indeed the resistance underwent several changes in resistance and these were not located at a precise voltage. Plus the resistance at the beginning and the end of the sweeping were not the same. In fact, we only had such results with the copper sample, letting us hope for more obvious bipolar switches in the future. The AlCu sample on the other hand, displayed the expected behavior for a bipolar resistive switching, so further investigation was led. We launched repeated measurements of the phenomenon, each time setting maximum amplitude of the switch just a little above the voltages we obtained for first switch (see figure 32).

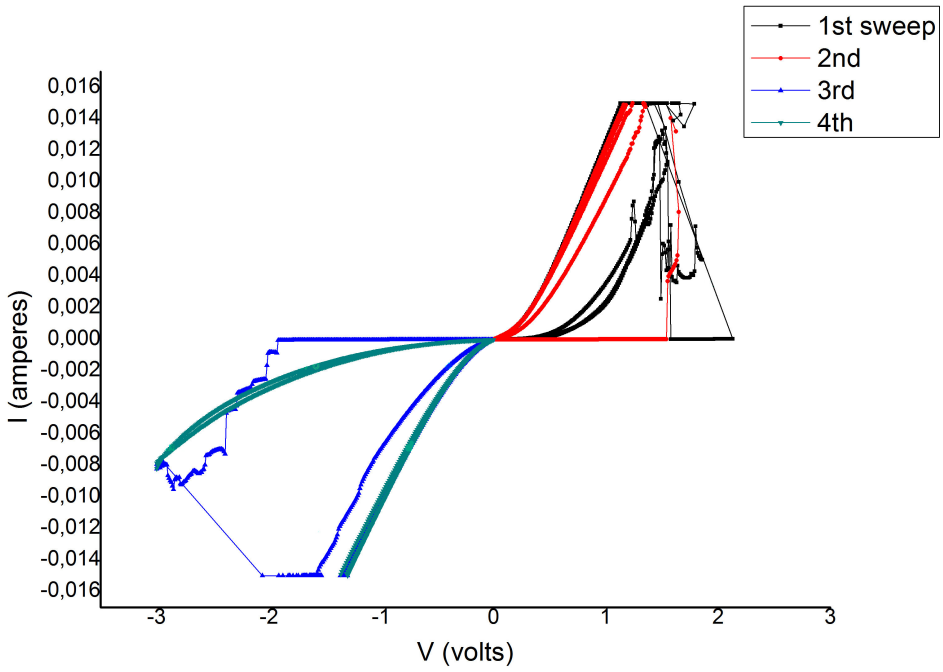

Figure 32: *Current induced against sweeping voltage on Alcu 130 nm device. Repeated tests*

On figure 32 above we can see a compliance current set at +-0,015 A which limits the current running in the device to allow to increase gradually the voltage to identify precisely a switching mechanism

Repeated cycling of sweeping voltages were set to see if we were witnessing a **reproducible phenomenon**. The repeated tests did not allow us to conclude to a reproducible switching mechanism. However, AlCu 130 nm top electrode devices showed promising behaviour for a further research in the field.

Conclusions and future prospects

In this work, we tried to develop graphene oxide based non volatile resistive memories. These memories are under research & development nowadays, and seem very promising, but the physics of the phenomenon remains unclear so far.

This work was really interesting and educative, since I was involved in two fabrication steps, spraying and photolithography, as well as sophisticated measurement instruments like atomic force microscope or electric characterizations. So it was a whole overview of the different steps in the making of such devices. The real challenge of the internship was that I had to deal with all these steps together, everyone of them having influence on the successive ones.

My work finds its reason to be in the precise fact that it allowed gathering many information elements about the beginning of this research activity. In the first part of the work, we established a process to deposit graphene oxide in a controlled way. Then we tried to take a closer insight in the complexity of the phenomena at stake in these devices, and to recognize already observed and understood patterns. We were lucky enough to find some switching mechanisms, in the devices with the electrochemically active top-electrodes, but not to find a reproducible phenomenon.

The follow-up of the work will probably consist in investigating the phenomena inside the graphene oxide layer, using observation instruments like XPS. Indeed for example in the work of Hong et al., such measurements were able to give important information about the top electrode diffusion, even though they are expensive to carry out. Another lead for improving the work would be to master photolithography better. The work being composed of many steps and this one being one of the steps that was less controlled.

Acknowledgements

I want to thank here everyone who has played a part in this work. Either people whom I studied and worked with, or more generally the ones who have helped or advised me.

I want to thank Paolo Bondavalli, my supervisor at Thales / CNRS for being welcoming, enthusiastic, and helpful in his guidance. I also want to thank Julie Grollier for her participation.

I want to thank Riccardo Bertacco, my supervisor for the Politecnico di Milano, for his help in the last part of my studies.

I want to thank all of the Nanocarb team, who were very welcoming and have managed to make their workplace in Palaiseau a very efficient and humane one.

I want to thank Gaëlle Lehoucq, for her disponibility and advices.

I want to thank all the other people who made my internship a very instructive time.

I want to thank all of my classmates and friends at Politecnico di Milano, particularly Antonio, for all the advices, help and good times spent together.

I want to thank my roommates Camillo, Erica, and Nicoletta for giving these years in Milan a daily rhythm and a particular taste.

I want to thank all the people I had the fortune to meet in Milan for making these three years a very enriching and meaningful experience.

Bibliography

[1] Standley B., Bao W., Zhang H. Bruck J., Ning Lau C., Bockrath M., 2008, « Graphene-Based Atomic-Scale Switches », *Nanolett*. 8, 10, 3345-3349

[2] Waser R., Dittmann R., Staikov G., Szot K., 2009, "Redox-Based Resistive Switching Memories", *Advanced Materials*, 21, 2632-2663

[3] Waser R., Aono M., 2007, « Nanoionics-based resistive switching memories », *Nature Materials* 6 11 833 840 1476-1122

[4] He H., Klinowski J., Forster M., Lerf A., 1998, « A new structural model for graphite oxide », *Chemical Physics Letters* 287 53

[5] Dreyer D., Park S., Bielawski C., Ruoff R., 2010, « Chemical Society Reviews », 39, 228-240

[6] Hong S.K., Kim J.E., Kim S.O., Cho B.J., 2011, « Journal of Applied Physics », 110, 4, 044506

[7] He C.L., Zhuge F., Kim S.O., Zhou X.F., Li M., Zhou G.C., 2009, « Applied Physics Letters», 95, 232101

[8] « Method for depositing nanoparticles on a surface and corresponding nanoparticle depositing appliance », patent deposited at INPI (France) in October 2010, FR2966062A1

[9] « Etude et réalisation des transistors à nanotubes de carbone pour la détection sélective de gaz », Louis Gorintin, Ph.D. work, 2011, Ecole Polytechnique

[10] Bondavalli P., Delfaure C., Legagneux P., Pribat D., 2013, « Supercapacitor electrode based on mixtures of graphite and carbon nanotubes deposited using a dynamic air-brush deposition technique », Journal of the Electrochemical Society, 160 (6), A1-A6

[11] « Dépôt et photogravure des couches minces », A. Vapaille, Université Paris-Sud, Institut d'Electronique Fondamentale

[12] Jeong H., Yun K., Won K. and others, 2010, « Graphene oxide thin films for flexible non volatile memory », Nanoletters, 10 4381-4386

[13] Panin G., Kapitanova O., Lee S., Baranov A., and Kang T., 2011, « Resistive switching in Al/Graphene oxide/Al structures », Japanese Journal of Applied Physics, 50, 070110

Appendix

Method for estimating the graphene oxide thickness via a scratch test, and AFM image for roughness calculation

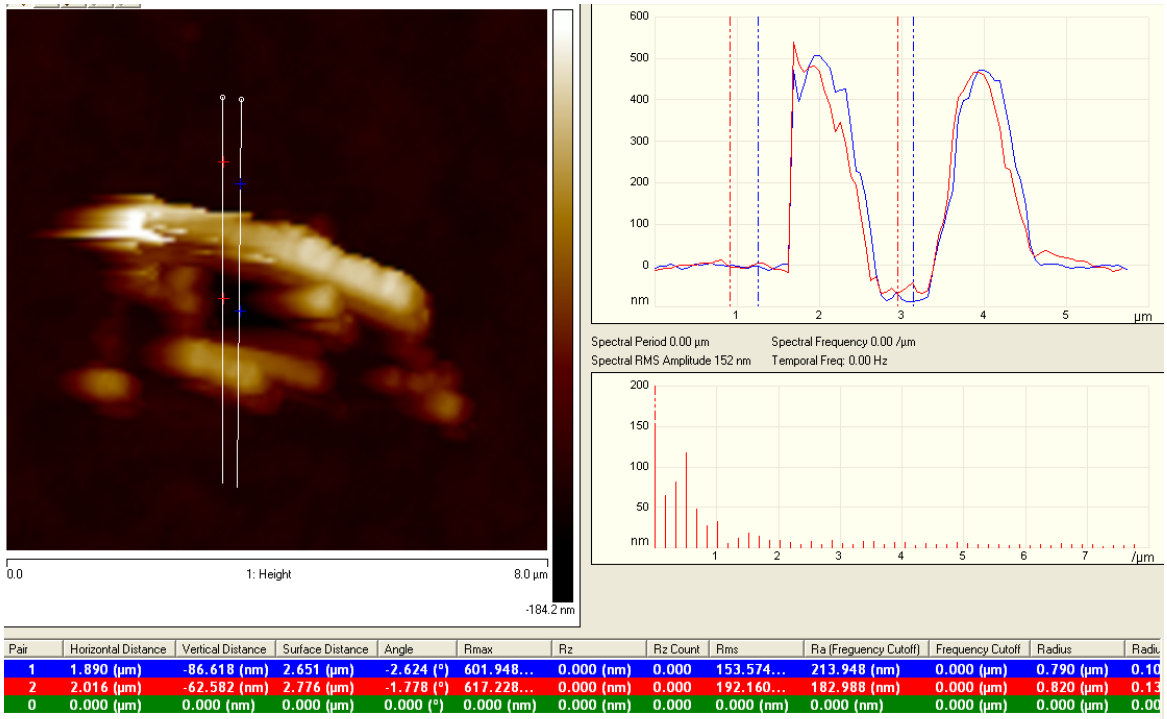

Pair	Horizontal Distance	Vertical Distance	Surface Distance	Angle	Rmax	Rz	Rz Count	Rms	Ra (Frequency Cutoff)	Frequency Cutoff	Radius	Radi
1	1.890 (µm)	-86.618 (nm)	2.651 (µm)	-2.624 (°)	601.948...	0.000 (nm)	0.000	153.574...	213.948 (nm)	0.000 (µm)	0.790 (µm)	0.10
2	2.016 (µm)	-62.582 (nm)	2.776 (µm)	-1.778 (°)	617.228...	0.000 (nm)	0.000	192.160...	182.988 (nm)	0.000 (µm)	0.820 (µm)	0.13
0	0.000 (µm)	0.000 (nm)	0.000 (µm)	0.000 (°)	0.000 (nm)	0.000 (nm)	0.000	0.000 (nm)	0.000 (nm)	0.000 (µm)	0.000 (µm)	0.00

AFM image of the scratched area and around for sample A
The height difference is read with the blue or red crosses

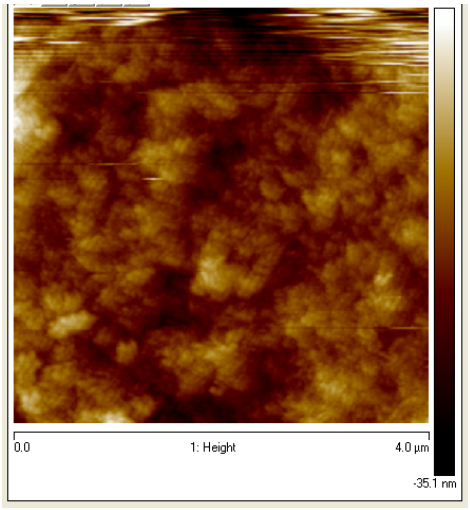

AFM image allowing the calculation of the roughness for sample A